NeuroImage: Clinical 19 (2018) 279–286

Contents lists available at ScienceDirect

NeuroImage: Clinical

journal homepage: www.elsevier.com/locate/ynicl

Brain function characteristics of chronic fatigue syndrome: A task fMRI study

Zack Y. Shan[a,*], Kevin Finegan[b], Sandeep Bhuta[b], Timothy Ireland[b], Donald R. Staines[a], Sonya M. Marshall-Gradisnik[a], Leighton R. Barnden[a]

[a] National Centre for Neuroimmunology and Emerging Diseases, Menzies Health Institute Queensland, Griffith University, Southport, QLD 4222, Australia
[b] Medical Imaging Department, Gold Coast University Hospital, Parklands, QLD 4215, Australia

ARTICLE INFO

Keywords:
Chronic fatigue syndrome
fMRI
Sample entropy
Stroop task
Event related fMRI

ABSTRACT

The mechanism underlying neurological dysfunction in chronic fatigue syndrome/myalgic encephalomyelitis (CFS/ME) is yet to be established. This study investigated the temporal complexity of blood oxygenation level dependent (BOLD) changes in response to the Stroop task in CFS patients.

43 CFS patients (47.4 ± 11.8 yrs) and 26 normal controls (NCs, 43.4 ± 13.9 yrs) were included in this study. Their mental component summary (MCS) and physical component summary (PCS) from the 36-item Short Form Health Survey (SF-36) questionnaire were recorded. Their Stroop colour-word task performance was measured by accuracy and response time (RT). The BOLD changes associated with the Stroop task were evaluated using a 2-level general linear model approach. The temporal complexity of the BOLD responses, a measure of information capacity and thus adaptability to a challenging environment, in each activated region was measured by sample entropy (SampEn).

The CFS patients showed significantly longer RTs than the NCs ($P < 0.05$) but no significant difference in accuracy. One sample *t*-tests for the two groups (Family wise error adjusted $P_{FWE} < 0.05$) showed more BOLD activation regions in the CFS, although a two sample group comparison did not show significant difference. BOLD SampEns in ten regions were significantly lower (FDR-q < 0.05) in CFS patients. BOLD SampEns in 15 regions were significantly associated with PCS (FDR-q < 0.05) and in 9 regions were associated with MCS (FDR-q < 0.05) across all subjects. SampEn of the BOLD signal in the medioventral occipital cortex could explain 40% and 31% of the variance in the SF-36 PCS and MCS scores, and those in the precentral gyrus could explain an additional 16% and 7% across all subjects.

This is the first study to investigate BOLD signal SampEn in response to tasks in CFS. The results suggest the brain responds differently to a cognitive challenge in patients with CFS, with recruitment of wider regions to compensate for lower information capacity.

1. Introduction

Chronic fatigue syndrome (CFS)/myalgic encephalopathy (ME) is characterized by a lasting and debilitating fatigue and affects 0.4–1% of the general population worldwide (Holgate et al., 2011). The pathology of CFS is yet to be established. It is believed that central nervous system (CNS) dysfunction plays an important role in CFS given well documented autonomic nervous system disorders, sleep disorders, attention deficits, impaired cognition, and reduced information processing speed (Holgate et al., 2011).

The brain structural changes associated with CFS have been extensively studied using quantitative magnetic resonance imaging (MRI) (Barnden et al., 2015; Barnden et al., 2011; Cook et al., 2001; Keenan, 1999; Lange et al., 1999; Lange et al., 1998; Perrin et al., 2010; Puri et al., 2012; Shan et al., 2016, 2017; Zeineh et al., 2015). These CFS structural neuroimaging results are somewhat inconsistent. One study reported loss in total grey matter (GM) (de Lange et al., 2005) while other studies found no significant difference (Barnden et al., 2011; Shan et al., 2016; Zeineh et al., 2015). Widely distributed structural changes have been reported in GM in prefrontal areas (Okada et al., 2004), the medial prefrontal cortex (Shan et al., 2017), and the occipital lobe, right angular gyrus, and the left parahippocampal gyrus (Puri et al., 2012); and in white matter (WM) in the left inferior fronto-occipital fasciculus (Shan et al., 2016), midbrain (Barnden et al., 2011), and right arcuate fasciculus (Zeineh et al., 2015) in CFS patients. Thus, subtle and distributed structural changes exist in CFS. Although their

* Corresponding author.
E-mail address: z.shan@griffith.edu.au (Z.Y. Shan).

https://doi.org/10.1016/j.nicl.2018.04.025
Received 1 November 2017; Received in revised form 14 March 2018; Accepted 22 April 2018
Available online 25 April 2018

functional consequences are unclear, indirect evidence for altered functional connectivity within the brainstem and hypothalamus has been reported (Barnden et al., 2016).

Recently brain function in CFS has been studied using functional MRI (fMRI) (Boissoneault et al., 2016a; Boissoneault et al., 2016b; Caseras et al., 2008; Cook et al., 2007; de Lange et al., 2004; Gay et al., 2016; Kim et al., 2015; Lange et al., 2005; Mizuno et al., 2016; Mizuno et al., 2015; Tanaka et al., 2006; Wortinger et al., 2016; Wortinger et al., 2017). Abnormal resting state brain connectivity was reported in several brain networks (Boissoneault et al., 2016a; Boissoneault et al., 2016b; Gay et al., 2016; Kim et al., 2015; Wortinger et al., 2016; Wortinger et al., 2017). In a few task fMRI (tfMRI) studies, motivation disturbance (de Lange et al., 2004; Mizuno et al., 2016), wider area of activated frontal regions (Mizuno et al., 2015), attenuated responsiveness of task-dependent brain regions (Tanaka et al., 2006), exaggerated emotional response (Caseras et al., 2008), and greater activity in several cortical and subcortical regions (Cook et al., 2007) were reported. Mizuno et al. (2015) argued that the greater and wider BOLD activation in CFS is likely to be less efficient and more costly in terms of energy requirement, causing a further increase in fatigue. However, the biological underpinning of the greater and wider BOLD activation in CFS remains elusive.

Temporal complexity is a fundamental feature of dynamic biological systems, such as is described by BOLD signals, and can be measured by the sample entropy (SampEn). Entropy is a measure of disorder or energy dispersal in classic physics. In information theory, entropy is defined as the amount of information produced by a probabilistic stochastic source of data. To better understand complex phenomena in biological time series, Pincus (2006) proposed approximate entropy, a measure of regularity closely related to Kolmogorov entropy, the rate of new information generation. Approximate entropy was further developed into the SampEn to reduce bias caused by self-match counting (Richman and Moorman, 2000). There has been increasing interest in measuring the SampEn in biological time series because it reflects the information capacity of the biological system and its adaptability to a changing environment (Goldberger et al., 2002; Hager et al., 2017). For example, an age-related loss in SampEn has been observed in BOLD signal fluctuation (Sokunbi, 2014), EEG recording (Takahashi et al., 2009), and magnetoencephalography (MEG) signals (Kielar et al., 2016). Given the wider activation and increased BOLD response during tasks in patients with CFS (Cook et al., 2007; Mizuno et al., 2015), we hypothesized that the SampEn of BOLD responses during tasks in patients with CFS would be different from normal controls (NCs).

2. Material and methods

2.1. Subjects

This study was approved by the Human Research Ethics Committees of the Griffith University and the Gold Coast University Hospital where scanning was performed. Signed informed consent was obtained from all participants. The Fukuda (Fukuda et al., 1994) diagnostic criteria were used to determine the existence of CFS. MRI scans were acquired for 83 subjects. 7 of these were excluded because they were taking central nervous system (CNS) medication or medication known to affect cerebral hemodynamic responses such as Indomethacin. A further four subjects did not meet the full Fukuda selection criteria (Fukuda et al., 1994) and three subjects with body mass index (BMI) higher than 35 were excluded. The total number of subjects analysed in this study was 69, comprised of 43 CFS patients and 26 normal controls (Table 1). We did not discriminate on the basis of gender during subject recruitment. Therefore, there were more females than males due to the gender difference in CFS incidence (Reyes et al., 2003). The NCs were recruited to match age and female-to-male ratio in the CFS group. All participants completed the 36-item Short Form Health Survey (SF-36) questionnaire (Ware et al., 1995), in which higher scores suggest better health.

Table 1
Demographics and Stroop task performance[a].

Parameters	CFS mean (SD)	NC mean (SD)	*P*
N	43	26	n/a
Female/male	31/12	18/8	n/a
Age (yrs.)	47.39 (11.81)	43.44 (13.93)	0.23
BMI	26.05 (5.04)	24.83 (3.52)	0.24
SF-36 PCS	29.97 (16.31)	93.12 (6.39)	< 0.001
SF-36 MCS	37.73 (20.21)	85.16 (9.78)	< 0.001
Heart rate (s^{-1})	1.6 (0.38)	1.59 (0.37)	0.9
Pulse pressure	0.81 (0.29)	0.72 (0.35)	0.26
Stroop task performance			
ACC_Con	0.95 (0.12)	0.98 (0.03)	0.2
ACC_Inc	0.89 (0.15)	0.91 (0.08)	0.58
ACC_Neu	0.96 (0.15)	0.99 (0.02)	0.29
RT_Con (s)	1.64 (0.57)	1.37 (0.31)	0.01
RT_Inc (s)	1.79 (0.52)	1.55 (0.35)	0.02
RT_N (s)	1.44 (0.37)	1.24 (0.26)	0.01
Stroop effect (%)	10 (12.39)	12.8 (9)	0.28

[a] SD = standard deviation; BMI = body mass index; n/a = not applicable; SF-36 PCS = physical component summary from 36-Item Short Form Health Survey (SF-36); SF-36 MCS = mental component summary from SF-36; ACC = accuracy; Con = congruent task; Inc = incongruent task; Neu = neutral task; RT = response time.

2.2. MRI acquisition

The MRI data were acquired on a 3T MRI scanner (Skyra, Siemens) while the subject viewed a video screen through goggles. Three dimensional T1-weighted anatomical images were acquired using a T1-weighted magnetization prepared rapid gradient-echo sequence (208 slices, repetition time (TR) = 2400 ms, echo time (TE) = 1.81 ms, flip angle = 8°, acquisition matrix = 224 × 224, voxel size 1 mm × 1 mm × 1 mm). The fMRI data were acquired using a multiband echo-planar imaging (EPI) pulse sequence developed at the University of Minnesota (Auerbach et al., 2013) (72 slices, multiband factor = 8, TR = 798 ms, TE = 30 ms, flip angle = 40°, acquisition matrix = 106 × 106, voxel size 2 mm × 2 mm × 2 mm). Before each fMRI data acquisition, a single band reference EPI volume and two spin echo EPI volumes encoded with opposite phase directions were acquired. 1100 tfMRI volumes were acquired over 15 min while the subject was performing a sequence of Stroop tasks. Physiological (respiratory and pulse oximetry) data were collected simultaneously with tfMRI data using the integrated Siemens physiological monitoring system.

2.3. Stroop task experimental paradigm

The subjects performed a randomized event-related colour word variant of the Stroop task during tfMRI acquisition (Leung et al., 2000). The Stroop task was selected because of the attention and concentration difficulties frequently reported by CFS patients (Ray et al., 1993). The participant was instructed to decide whether the colour of the upper word agreed with the meaning of the lower word and press one of two buttons on a handpiece accordingly. The upper word, consisting of either RED, BLUE, YELLOW, or XXXX, was presented in colours of red, blue, or yellow on a black background. The lower word was either RED, BLUE, or YELLOW coloured white on a black background (Supplementary Fig. S1). 110 trials were randomly distributed over a session of 15 min with averaged interstimulus time of 10.5 s. Among them, 40% of the trials were incongruent (e.g. upper word RED written in blue), 30% congruent (e.g. BLUE written in blue), and 30% neutral (e.g. XXXX written in yellow). The Stroop paradigm was encoded using Cogent (The Laboratory of Neurobiology, www.vislab.ucl.ac.uk). The time of stimulus-ON, the response time (RT), and the accuracy were recorded for each subject. The Stroop effect was calculated as the average RT of incongruent trials minus the average RT of congruent trials normalized to the average RT of all trials.

2.4. MRI pre-processing

The tfMRI data were pre-processed as follows. (1) The first five of the 1100 fMRI EPI volumes were discarded to ensure that tissue magnetization had reached steady state. (2) Motion correction was applied by registering 1095 EPI volumes to the single band reference image acquired immediately before them using MCFLIRT (Jenkinson et al., 2002) implemented in FSL (FMRIB's Software Library, www.fmrib.ox.ac.uk/fsl). (3) A distortion correction was applied using the distortion field calculated from the two oppositely phase-encoded spin echo EPI volumes using the toolbox "topup" (Andersson et al., 2003) implemented in FSL. (4) The distortion corrected fMRI volumes were coregistered to the corresponding T1 3D anatomic image and then spatially normalized to the Montreal Neurological Institute (MNI) space average brain T1 template (Ashburner and Friston, 1999) using SPM12 (Wellcome Trust Centre for Neuroimaging, London, UK). (5) Normalized volumes were smoothed with a $4 \times 4 \times 4\,mm^3$ full width at half maximum Gaussian kernel using SPM12.

2.5. Physiological data processing

The physiological data were processed using an in-house MATLAB program to detect peaks and troughs in pulse oximetry recordings and reject peaks that yielded outlier peak-to-peak intervals. The heart rate (HR) was calculated as the reciprocal of the peak-to-peak time and relative pulse pressure (PP) as the amplitude difference between a peak and the preceding trough. HR and PP were then interpolated to yield values for each fMRI volume to be used as covariates in general linear modelling (GLM) of the BOLD activation map in SPM12.

2.6. BOLD changes associated with Stroop task

The tfMRI data were analysed using the two level GLM approach implemented in SPM12. At the subject level, the activation map associated with each trial and the difference between task and rest periods were determined by correlating the BOLD response with the convolution of the HRF and the neural event as defined by the stimulus-on and subject response time. A canonical hemodynamic response function (HRF) with time and dispersion derivatives was used. The instantaneous HR and PP at each fMRI volume were included as covariates. The congruent, incongruent, neutral, 'Stroop' (incongruent – congruent), and task minus rest (positive) t-contrast maps were entered into a group-level analysis. At the group level, we performed random-effect one-sample *t*-tests to identify neural correlates of tasks in each group and two sample *t*-tests to identify group differences between CFS and NC ($\alpha < 0.05$ with family wise error (FWE) adjusted for multiple comparisons).

2.7. Extraction of brain structure fMRI time series

Brain structures where the BOLD signal significantly correlated with the task in the CFS and NC groups were identified with a brain atlas, derived from cytoarchitectonic, functional and structural connectivity information (Fan et al., 2016). The fMRI time series for structures that were activated in both groups were extracted using an in-house toolkit based on MATLAB and SPM12 functions. For each structure, for each subject, a region was defined by iterative exclusion at the voxel level based on self-coherence as follows. (1) With the initial region defined by overlap of the group activation map and the atlas, an fMRI time series for the region was extracted by averaging the signal intensity in all voxels within the region at each time point. (2) For each voxel within the region, the correlation between the voxel time series and the region time series was calculated. (3) The voxels that were not significantly correlated ($P > 0.05$) were excluded, then the average region time series was calculated again. (4) Steps (1) to (3) were repeated until no more voxels were excluded. The fMRI time series for each brain structure was then extracted and smoothed with a high pass filter of 128 s to remove baseline drift.

2.8. Temporal complexity (SampEn)

SampEn was used to measure the temporal complexity of each time series (Richman and Moorman, 2000). The MATLAB function for SampEn calculation was downloaded from the PhysioNet (www.physionet.org/physiotools/sampen/). Given a full time series of data with length N, the SampEn was calculated as the negative natural logarithm of the probability that segments of data points with length m, $X_m(i) = \{x_i, x_{i+1}, x_{i+2}, \ldots, x_{i+m-1}\}$, that are similar within a tolerance r, remain similar when the segments were extended to include the next data point (Eq. (1)).

$$SampEn = -\ln \frac{C_{m+1}}{C_m}, \tag{1}$$

where C_m is the count of data segments with length m having the Chebyshev distance d smaller than the tolerance r. For a segment $X_m(i)$, the Chebyshev distance d was defined in Eq. (2),

$$d[X_m(i), X_m(j)]\,(i \neq j) = \underbrace{max}_{i}(|x_i - x_j|). \tag{2}$$

In this study, the length m was set to 3 and the tolerance r was set to 0.2 times of the standard deviation of the full time series.

2.9. Statistical analysis

For structures where the BOLD signal significantly correlated with the task, differences between CFS and NC groups in clinical variables and in the SampEns were compared using the independent-samples *t*-Test in SPSS22 (IBM, New York). The P values of SampEns were converted into false discovery rate probabilities (FDR-Q) using the R (www.r-project.org) code proposed by Benjamini and Hochberg (1995) for multiple comparison correction. FDR-Q < 0.05 was considered as statistically significant. Significantly different SampEns were further analysed using GLM univariate analysis in SPSS to exclude age and body mass index (BMI) confounds. In the univariate analysis, each SampEn was entered as a dependent variable; the group (CFS or NC) was entered as a fix factor; the age and the BMI were entered as covariates. The group difference in SampEn was estimated with adjustment for age and BMI. The Pearson correlation was used to determine correlations between clinical variables and SampEns across all subjects followed by a conversion to FDR-Q values. The variables that were significantly correlated with health scores (significance threshold FDR-Q < 0.05) were further analysed using a hierarchical regression analysis to determine if those measures contributed to variance in the health scores across all subjects. In each hierarchical regression, the PCS and MCS were entered as dependent variables; the demographic data including age, HR, PP, and BMI were entered as first block independent variables with the forced entry method; the SampEns of BOLD signals were entered as second block independent variables with the stepwise entry method.

3. Results

3.1. Demographics and behaviour findings

Table 1 shows no significant difference in BMI, HR, or PP between the CFS and NC groups. The physical component summary (PCS) and mental component summary (MCS) scores from the SF-36 survey (Ware et al., 1995) in CFS were significantly lower than those in NCs (Table 1). In the Stroop task the CFS patients scored a slightly lower accuracy and showed less Stroop effect than NCs, but the difference was not significant. However, the RT of CFS patients was significantly longer than NCs (Table 1).

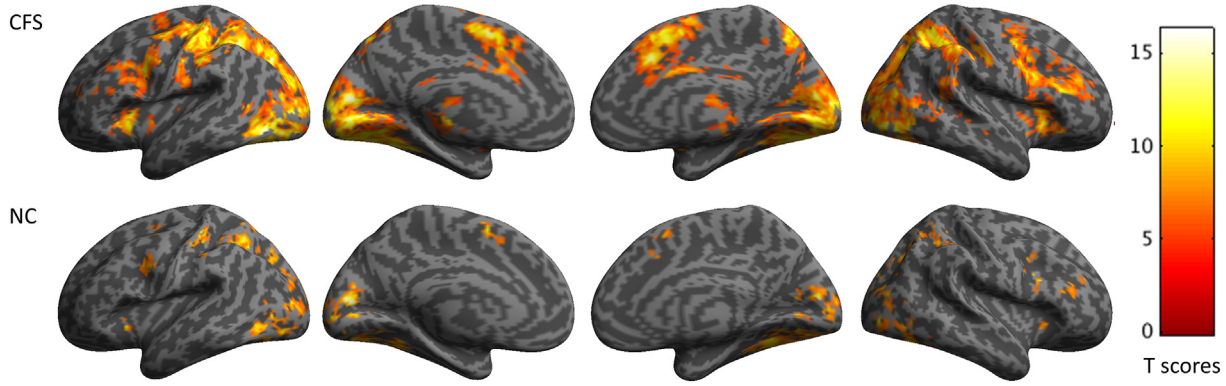

Fig. 1. Group level BOLD signal changes associated with the Stroop task. From left to right are shown average activations from the left lateral and medial views of the left hemisphere and the medial and right lateral views of the right hemisphere. The group level activation maps show that the CFS patients had more extended positive BOLD responses (top row) than the NCs (bottom row).

3.2. BOLD changes associated with Stroop task

The group-level one sample *t*-test BOLD responses associated with the Stroop task were mapped in Montreal Neurological Institute (MNI) space (Fig. 1). These show that CFS patients have larger regions with greater blood flow when engaging in the Stroop task than NCs. The regions activated during the task were identified using a connectivity based brain atlas which includes 210 cortical and 36 subcortical structures (Fan et al., 2016). There were 50 areas activated in both the CFS and NC groups (Table 2). There were 93 brain areas activated exclusively in the CFS group. They included regions in the superior frontal gyrus, middle frontal gyrus, inferior frontal gyrus, precentral gyrus, superior temporal gyrus, middle temporal gyrus, inferior temporal gyrus, parahippocampal gyrus, posterior superior temporal sulcus, superior parietal lobule, inferior parietal lobule, precuneus, postcentral gyrus, insular gyrus, cingulate gyrus, lateral occipital cortex, amygdala, hippocampus, basal ganglia, and thalamus (Supplementary Table S1). Only one region was exclusively activated for the NC group: the right A37elv (extreme lateroventral area 37) in the inferior temporal gyrus. However, the two sample *t*-test comparing individual contrast maps from CFS and NCs was not significant.

3.3. SampEn of BOLD signals

The SampEns of BOLD signals in 10/50 areas activated in both CFS and NCs were significantly lower in CFS patients (Table 3). The significance levels remained unchanged or slightly improved after adjusting for ages and BMIs. The SampEns of the remaining 40 regions

Table 3
Different SampEns of BOLD signals between CFS patients and NCs[a].

Areas	CFS mean (SD)	NC mean (SD)	*P*	FDR-Q	*P**
L A6m_ SFG	1.81 (0.16)	1.94 (0.15)	0.001	0.01	0.001
R IFJ_MFG	1.71 (0.2)	1.85 (0.16)	0.003	0.02	0.001
L A6cdl_PrG	1.77 (0.16)	1.93 (0.18)	< 0.001	0.003	< 0.001
L A6cvl_PrG	1.62 (0.16)	1.76 (0.17)	0.001	0.007	0.001
R A6cvl_PrG	1.62 (0.19)	1.79 (0.15)	< 0.001	0.003	< 0.001
R A40rd_IPL	1.55 (0.22)	1.73 (0.2)	0.001	0.007	< 0.001
L cLinG_MVOcC	1.75 (0.23)	1.92 (0.16)	0.002	0.01	0.001
L rLinG_MVOcC	1.9 (0.15)	2.03 (0.12)	< 0.001	0.005	< 0.001
R vmPOS_MVOcC	1.83 (0.15)	2.01 (0.12)	< 0.001	0.001	< 0.001
R OPC_LOcC	1.7 (0.19)	1.84 (0.22)	0.008	0.04	0.005

[a] BOLD = blood oxygenation level dependent, SampEn = sample entropy, CFS = chronic fatigue syndrome, NC = normal control, $Mean_{CFS}$ = mean value in the CFS group, $Mean_{NC}$ = mean value in the NC group, *P* = calculated probability in independent two sample *t*-test, FQR-Q = false discovery rate (FDQ) adjusted probability, *P** = calculated probability of group difference using SPSS GLM univariate analysis adjusted for age and BMI. L = left, R = right, A6m_SFG = medial area 6 in superior frontal gyrus, IFJ_MFG = inferior frontal junction in middle frontal gyrus, IFS_PrG = inferior frontal sulcus in precentral gyrus (PrG), A6cdl_PrG = caudal dorsolateral area 6 in PrG, A6cvl_PrG = caudal ventrolateral area 6 in PrG, A40rd_IPL = rostrodorsal area 40 in inferior parietal lobule, cLinG_MVOcC = caudal lingual gyrus in medioventral occipital cortex (MVOcC), rLinG_MVOcC = rostral lingual gyrus in MVOcC, vmPOS_MVOcC = ventromedial parietooccipital sulcus in MVOcC, OPC_LOcC = occipital polar cortex in lateral occipital cortex (LOcC).

Table 2
Brain areas activated in both CFS patients and NCs[a].

Lobe	Gyrus	Cytoarchitectonic name
Frontal lobe	Superior frontal gyrus (SFG)	LR A8m (medial area 8); L A6m (medial area 6)
	Middle frontal gyrus (MFG)	R IFJ (inferior frontal junction); R A9/46v (ventral area 9/46); L A6vl (ventrolateral area 6)
	Inferior frontal gyrus (IFG)	R IFS (inferior frontal sulcus)
	Precentral gyrus (PrG)	L A6cdl (caudal dorsolateral area 6); LR A6cvl (caudal ventrolateral area 6)
Temporal lobe	Inferior temporal gyrus (ITG)	L A37elv (extreme lateroventral area 37);
	Fusiform gyrus (FuG)	R A20rv (rostroventral area 20); LR A37mv (medioventral area 37); LR A37lv (lateroventral area 37)
Parietal lobe	Superior parietal lobule (SPL)	R A7c (caudal area 7); L A5l (lateral area 5), LR A7ip (intraparietal area 7, hIP3);
	Inferior parietal lobule (IPL)	LR A39c (caudal area 39, PGp); LR A39rd (rostrodorsal area 39, Hip3); LR A40rd (rostrodorsal area 40, PFt);
	Postcentral gyrus (PoG)	L A2, area 2
Insular lobe	Insular gyrus (INS)	LR dIa (dorsal agranular insula)
Limbic lobe	Cingulate gyrus (CG)	R A32p (pregenual area 32)
Occipital lobe	Medioventral occipital cortex (MVOcC)	LR cLinG (caudal lingual gyrus); LR rCunG (rostral cuneus gyrus); LR cCunG (caudal cuneus gyrus); LR rLinG (rostral lingual gyrus); LR vmPOS (ventromedial parietooccipital sulcus)
	Lateral occipital cortex (LOcC)	LR mOccG (middle occipital gyrus); LR V5/MT+ (area V5/MT+); LR OPC (occipital polar cortex); LR iOccG (inferior occipital gyrus); LR lsOccG (lateral superior occipital gyrus)

[a] CFS = chronic fatigue syndrome; L = left; R = right; LR = left and right.

Table 4
Significant correlations between BOLD signal SampEns and health scores across all subjects[a].

Areas	SF-36 PCS			SF-36 MCS		
	r	*P*	FDR-Q	*r*	*P*	FDR-Q
L A6m	0.38	0.003	0.02	0.34	0.007	0.04
R IFJ	0.36	0.005	0.03	0.28	0.03	0.09
L A6cdl	0.45	< 0.001	0.004	0.37	0.004	0.04
L A6cvl	0.5	< 0.001	0.001	0.37	0.003	0.04
R A6cvl	0.43	0.001	0.006	0.28	0.03	0.09
R A37mv	0.34	0.008	0.03	0.26	0.04	0.12
R A39c	0.37	0.004	0.02	0.35	0.006	0.04
R A40rd	0.34	0.009	0.03	0.33	0.01	0.05
L cLinG	0.31	0.02	0.05	0.17	0.19	0.29
L rLinG	0.45	< 0.001	0.004	0.35	0.006	0.04
R vmPOS	0.59	< 0.001	< 0.001	0.59	< 0.001	< 0.001
L mOccG	0.32	0.01	0.04	0.24	0.07	0.16
R V5/MT+	0.38	0.003	0.02	0.34	0.007	0.04
R OPC	0.36	0.006	0.03	0.35	0.006	0.04
L lsOccG	0.33	0.01	0.04	0.28	0.03	0.09

[a] BOLD = blood oxygenation level dependent, SampEn = sample entropy, SF-36 PCS = physical component summary in 36-item Short Form Health Survey (SF-36), SF-36 MCS = mental component summary in SF-36, *r* = Pearson correlation coefficient, *P* = calculated probability in Pearson correlation, FQR-Q = false discovery rate (FDQ) adjusted probability, L = left, R = right, A6m_SFG = medial area 6 in superior frontal gyrus, IFJ = inferior frontal junction in middle frontal gyrus, A6cdl = caudal dorsolateral area 6 in precentral gyrus (PrG), A6cvl = caudal ventrolateral area 6 in PrG, A37mv = medioventral area 37 in fusiform gyrus, A39c = caudal area 39 in inferior parietal lobule (IPL), A40rd = rostrodorsal area 40 in IPL, cLinG = caudal lingual gyrus in medioventral occipital cortex (MVOcC), rLinG = rostral lingual gyrus in MVOcC, vmPOS = ventromedial parietooccipital sulcus in MVOcC, mOccG = middle occipital gyrus in lateral occipital cortex (LOcC), V5/MT+ = area V5/MT+ in LOcC, OPC = occipital polar cortex in LOcC, lsOccG = lateral superior occipital gyrus in LOcC.

were not significantly different and are summarised in Supplementary Table S2.

3.4. SampEn of BOLD signals correlated with health scores

The SampEns of BOLD signals in 15 areas were significantly (FDR-Q < 0.05) correlated with SF-36 PCS and in 9 areas were significantly (FDR-Q < 0.05) correlated with SF-36 MCS (Table 4) across all subjects. Seven areas in which the SampEns of the BOLD signal were significantly lower in CFS and significantly correlated with both PCS and MCS scores across all subjects are shown in Fig. 2.

3.5. SampEn of BOLD signals accounts for variances of health scores

The SampEns of BOLD signals in the R vmPOS of the MVOcC accounted for 40% of variance in the SF-36 PCS and SampEns in the L A6cvl of the PrG accounted for an additional 16% (Table 5) in all subjects. The SampEns of BOLD signals in the R vmPOS of the MVOcC accounted for 31% variances in the SF-36 MCS and those in the L A6cvl of the PrG accounted for an additional 7% across all subjects (Table 6).

4. Discussion

The aim of this study was to investigate whether the brain operates differently in patients with CFS. We found that CFS patients took longer to respond to the Stroop task although the accuracy of their response was similar to NCs. The one sample *t*-test for BOLD correlations with task showed that CFS patients recruit more regions for the Stroop task (Fig. 1) although a two-sample (CFS vs. NC) t-test did not show a significant difference. The SampEns of BOLD signals were significantly lower in 10 structures in CFS patients. The SampEns were significantly correlated with the PCS heath scores in 15 areas and with the MCS score in 9 areas across all subjects. Fig. 2 illustrates 7 areas in which the SampEns of the BOLD signal were significantly lower in CFS and significantly correlated with both PCS and MCS scores. SampEn in the R vmPOS of the MVOcC accounted for 40% and 31% of the PCS and MCS score variances and SampEn in the L A6cvl of the PrG accounted for an additional 16% and 7% in all subjects.

Previous studies have shown that CFS patients recruit wider regions with greater BOLD activation in response to motor imagery tasks (de Lange et al., 2004), 2- and 3-back working memory tasks (Caseras et al., 2006), auditory monitoring tasks(Cook et al., 2007), and Kana Pick-out Test tasks (Mizuno et al., 2015). Our GLM one sample t-test results are consistent with these studies (Fig. 1), i.e. CFS patients recruit more BOLD activation regions and need a longer time to accomplish tasks with similar accuracies. However, our two sample comparison between CFS patients and NCs did not show any significant difference. We postulate that this negative two sample t-test result could be attributed to the lower detection power of our fMRI paradigm, a slow (averaged interstimulus time of 10.5 s) randomized event-related fMRI design. To investigate whether the brain operates differently, instead of simply confirming previous findings of wider neural correlates for tasks in CFS, this study used a slow randomized event-related paradigm for its optimal capability in detecting transient variations in hemodynamic impulse in response to tasks (Liu et al., 2001; Tie et al., 2009).

This study observed that CFS patients recruited the additional subcortical structures of amygdala, hippocampus, basal ganglia, and thalamus in response to the Stroop tasks. The well-documented brain areas that respond to the Stroop task are mainly cortical regions including the anterior cingulate cortex, insula, frontal, parietal, and occipital regions, and/or thalamus but not including the hippocampus and basal ganglia (Coste et al., 2011; Leung et al., 2000). A previous study of an auditory monitoring task observed that CFS patients also recruited the hippocampus and thalamus subcortical structures (Cook et al., 2007). The exaggerated BOLD responses in CFS patients in response to cognitive tasks would contribute to fatigue, if not constitute its cause. However, the reason why CFS patients recruit wider BOLD activations in response to cognitive tasks has remained elusive.

This study found that the SampEn of the BOLD time series in a Stroop task fMRI is lower in 10 areas in CFS patients. The unchanged or slightly increased significance level after adjusting for age and BMI indicated that the lower SampEn was not attributable to age or BMI differences. The BOLD signal is a convolution of neural activity and hemodynamic response function (HRF). Biologically, variation in the BOLD response is mainly affected by neural activity, neurovascular coupling, cerebral blood flow, and/or noise. Given that fMRI data from CFS patients and NCs were here acquired and processed in the same way and that BOLD SampEn is lower in only 10 of 50 common activation areas, we argue that the lower SampEn in CFS patients is not likely attributable to global noise bias. The two studies of cerebral blood flow in CFS patients have been inconsistent, with one study showing no difference from NCs (Perrin et al., 2010) and the other showing a global decrease affecting all regions assessed (Biswal et al., 2011). However, we only observed lower BOLD SampEn in 10 from 50 areas. Furthermore, the HR and PP, collected simultaneously with fMRI, remained similar between CFS patients and NCs. Therefore, SampEn in these 10 areas in CFS patients is not likely to derive from baseline cerebral blood flow. The lower SampEn of BOLD signals observed here in 10 areas most likely indicates differences in neural responses and/or neurovascular coupling. This study is not able to distinguish between the two. However, a recent report of reduced expression of transient receptor potential melastatin subfamily 3 (TRPM3) protein in CFS patients (Nguyen et al., 2017) suggests neurovascular coupling may dominate. TRPM3, expressed both in the peripheral nervous system and the CNS, is a cell membrane channel with high Ca^{2+} permeability. Ca^{2+} participates in several major pathways regulating neurovascular

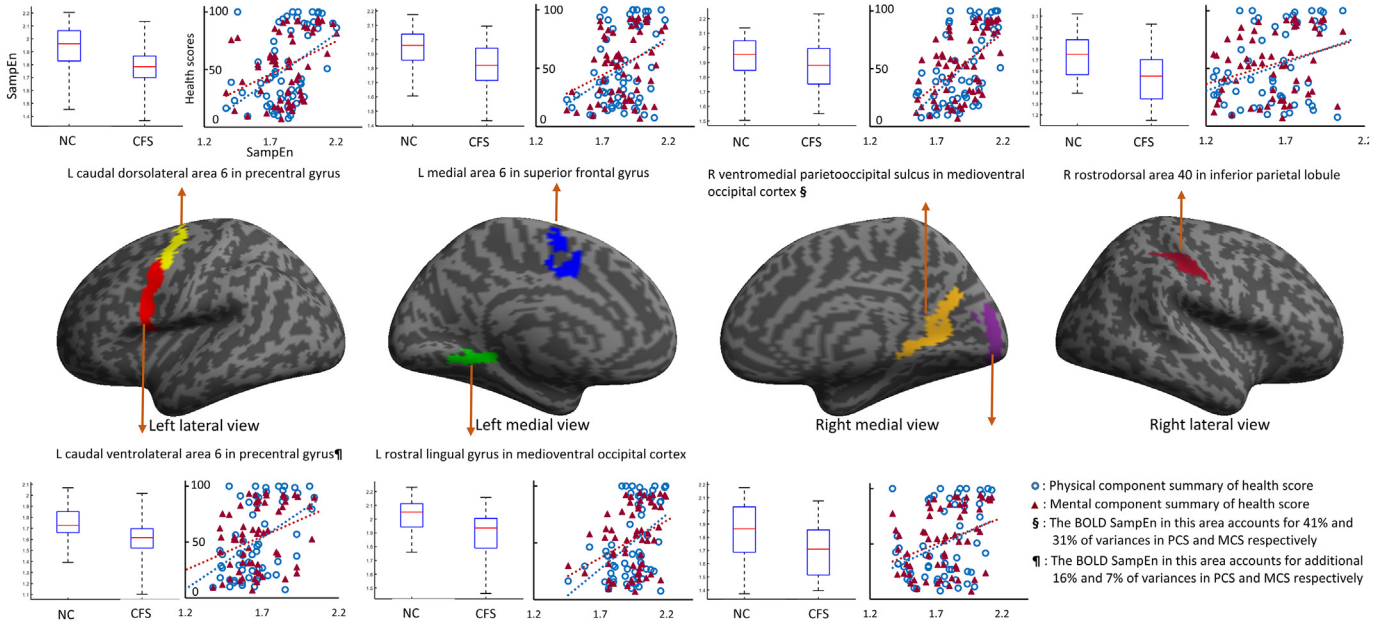

Fig. 2. Seven areas in which the sample entropy (SampEn) in CFS is lower than in NC and correlates with health scores. In these seven areas, the SampEns of BOLD responses to the Stroop tasks were significantly different (FDR-Q < 0.05, Table 3) between CFS patients and normal controls (NCs) and were significantly correlated (FDR-Q < 0.05, Table 4) with physical component summary (PCS) and mental component summary (MCS) scores from the 36-item Short Form Health Survey (SF-36) questionnaire. The boxplot depicts the median and interquartile range (IQR) of BOLD SampEn in each area with outliers determined by 3 times IQR. The scatter plots show the linear relationship between the CFS BOLD SampEn and PCS/MCS sores for each subject in each area.

Table 5
Hierarchical regression of SampEns predicting PCS health score across all subjects[a].

		b	*SE b*	*β*
Model 1	Constant	106.67	31.4	
	Age	−0.23	0.35	−0.09
	HR	6.04	13.87	0.07
	PP	−16.16	16.43	−0.16
	BMI	−1.65	0.98	−0.23
Model 2	Constant	−118.22	42.58	
	Age	−0.63	0.27	−0.24
	HR	−5.34	10.68	−0.06
	PP	−20.27	12.51	−0.2
	BMI	−1.02	0.75	−0.14
	$SampEn_{R\_vmPOS\_MVOcC}$	130.55	20.52	**0.67****
Model 3	Constant	−186.53	38.63	
	Age	−0.64	0.23	−0.25
	HR	−13.07	9.15	−0.15
	PP	−27.05	0.63	−0.26
	BMI	−1.06	0.63	−0.15
	$SampEn_{R\_vmPOS\_MVOcC}$	104.65	18.12	**0.53****
	$SampEn_{L\_A6cvl\_PrG}$	81.87	17.2	**0.45****

[a] $\Delta R^2 = 0.08$ for model 1, $\Delta R^2 = 0.4$ for model 2 (Significant F Change < 0.001), $\Delta R^2 = 0.16$ for model 3 (Significant F Change < 0.001); **: $P < 0.001$; SampEn = sample entropy, PCS = physical component summary in 36-item Short Form Health Survey, *b* = unstandardized coefficients, *SE b* = standard error of *b*, *β* = standardized coefficient, HR = heart rate, PP = pulse pressure, BMI = body mass index, $SampEn_{R\_vmPOS\_MVOcC}$ = SampEn of blood oxygenation level dependent (BOLD) signal in right ventromedial parietooccipital sulcus in medioventral occipital cortex, $SampEn_{L\_A6cvl\_PrG}$ = SampEn of BOLD signal in left caudal ventrolateral area 6 in precentral gyrus.

Table 6
Hierarchical regression of SampEns predicting MCS health score across all subjects[a].

		b	*SE b*	*β*
Model 1	Constant	70.47	27.33	
	Age	0.14	0.3	0.06
	HR	9.73	12.07	0.13
	PP	−15.28	14.3	−0.17
	BMI	−1.09	0.85	−0.17
Model 2	Constant	−98.97	40.57	
	Age	−0.16	0.26	−0.07
	HR	1.21	10.18	0.16
	PP	−18.39	11.92	−0.2
	BMI	−0.0.61	0.71	−0.1
	$SampEn_{R\_vmPOS\_MVOcC}$	98.58	19.55	**0.58****
Model 3	Constant	−136.68	41.84	
	Age	−0.17	0.25	−0.08
	HR	−3.11	9.91	−0.04
	PP	−22.13	11.51	−0.25
	BMI	−0.63	0.68	−0.1
	$SampEn_{R\_vmPOS\_MVOcC}$	84.29	19.63	**0.5****
	$SampEn_{L\_A6cvl\_PrG}$	45.18	18.62	**0.29***

[a] $\Delta R^2 = 0.05$ for model 1, $\Delta R^2 = 0.31$ for model 2 (Significant F Change < 0.001), $\Delta R^2 = 0.07$ for model 3 (Significant F Change < 0.05); *: $P < 0.05$, **: $P < 0.001$; SampEn = sample entropy, MCS = mental component summary in 36-item Short Form Health Survey, *b* = unstandardized coefficients, *SE b* = standard error of *b*, *β* = standardized coefficient, HR = heart rate, PP = pulse pressure, BMI = body mass index, $SampEn_{R\_vmPOS\_MVOcC}$ = SampEn of blood oxygenation level dependent (BOLD) signal in right ventromedial parietooccipital sulcus in medioventral occipital cortex, $SampEn_{L\_A6cvl\_PrG}$ = SampEn of BOLD signal in left caudal ventrolateral area 6 in precentral gyrus.

coupling (Attwell et al., 2010): (1) raised Ca^{2+} concentration ($[Ca^{2+}]$) in neurons releases the blood vessel dilator NO and possibly also generates arachidonic acid (AA) to produce prostaglandins (PG) that also dilate blood vessels; (2) raised $[Ca^{2+}]$ in astrocytes also generates AA to produce metabolites PG and epoxyeicosatrienoic acid (EETs) which dilate blood vessels; (3) raised $[Ca^{2+}]$ in astrocyte end feet may activate Ca^{2+}-gated K^+ channels, releasing K^+, which also dilates vessels.

The SampEn is a measure of the information carrying capability of the biological system, which in turn determines its adaptability to a changing environment (Goldberger et al., 2002; Hager et al., 2017). This study found that the brain BOLD signal response to the Stroop task in CFS patients resulted in lower SampEn. Our finding suggests that the

information carrying capability, i.e. neural activity and/or neurovascular coupling, is lower in CFS patients. Taken together, our results from GLM and SampEn measures suggest that the brain recruits wider regions in CFS patients to compensate for the lower information capacities in their BOLD responses.

This study investigated the SampEn of tfMRI time series, which was different from the SampEn of rsfMRI time series (Shan et al., 2018). A randomized event-related fMRI paradigm was used so that activated BOLD response in tfMRI time series did not influence SampEn evaluation. The SampEn of tfMRI signals in activated regions reflects the brain's adaptability to cognitive challenges, while rsfMRI signal fluctuation is believed to be driven by spontaneous background activity. One of our recent studies showed that the BOLD SampEn in the posterior cingulate cortex (PCC) is higher in CFS patients in both rsfMRI and tfMRI (Shan et al., 2018). The PCC is the primary and driving hub for spontaneous activity in the default mode network. Results from this study and our previous study (Shan et al., 2018) have therefore shown a BOLD signal variation pattern in CFS, lower BOLD SampEns in regions activated by randomized Stroop tasks and higher SampEns of spontaneous default mode network BOLD fluctuation.

This study had two limitations. First, there were fewer NCs than CFS patients due to the difficulty of recruiting age-matched normal subjects. Although several fMRI databases have become publically available, Stroop task fMRI data is not yet available. Second, this study observed lower BOLD SampEns in CFS in 10 brain regions but was not able to distinguish between neural responses or neurovascular coupling as its origin. A future study is planned to further investigate this process.

5. Conclusions

This study investigated BOLD responses to the Stroop task in CFS patients. We found that CFS patients recruit more regions to accomplish the Stroop task than controls. Among 50 regions with BOLD activation in both CFS patients and NCs, SampEns of BOLD signals in 10 areas were significantly lower in CFS patients and significantly correlated with health scores across all subjects. The SampEn of BOLD signals in the medioventral occipital cortex accounted for 40% and 31% of the variance in the SF-36 PCS and MCS scores respectively, and those in the precentral gyrus accounted for an additional 16% and 7% across all subjects. These findings indicate that the brain recruits wider regions to compensate for the lower information capacity of the BOLD responses in CFS.

Acknowledgement

We thank the patients and normal controls who donated their time and effort to participate in this study. This study was supported by the Stafford Fox Medical Research Foundation, the Judith Jane Mason Foundation (MAS2015F024), Mr. Douglas Stutt, and Blake-Beckett Foundation. The financial support did not affect any aspect of the study.

Declaration of interest

All the authors have no conflict of interests existed.

Appendix A. Supplementary data

Supplementary data to this article can be found online at https://doi.org/10.1016/j.nicl.2018.04.025.

References

Andersson, J.L., Skare, S., Ashburner, J., 2003. How to correct susceptibility distortions in spin-echo echo-planar images: application to diffusion tensor imaging. NeuroImage 20, 870–888.
Ashburner, J., Friston, K.J., 1999. Nonlinear spatial normalization using basis functions. Hum. Brain Mapp. 7, 254–266.
Attwell, D., Buchan, A.M., Charpak, S., Lauritzen, M., Macvicar, B.A., Newman, E.A., 2010. Glial and neuronal control of brain blood flow. Nature 468, 232–243.
Auerbach, E.J., Xu, J., Yacoub, E., Moeller, S., Ugurbil, K., 2013. Multiband accelerated spin-echo echo planar imaging with reduced peak RF power using time-shifted RF pulses. Magn. Reson. Med. 69, 1261–1267.
Barnden, L.R., Crouch, B., Kwiatek, R., Burnet, R., Mernone, A., Chryssidis, S., Scroop, G., Del Fante, P., 2011. A brain MRI study of chronic fatigue syndrome: evidence of brainstem dysfunction and altered homeostasis. NMR Biomed. 24, 1302–1312.
Barnden, L., Crouch, B., Kwiatek, R., Burnet, R., Del Fante, P., 2015. Evidence in Chronic Fatigue Syndrome for severity-dependent upregulation of prefrontal myelination that is independent of anxiety and depression. NMR Biomed. 28, 404–413.
Barnden, L., Kwiatek, R., Crouch, B., Burnet, R., Del Fante, P., 2016. Autonomic correlations with MRI are abnormal in the brainstem vasomotor centre in Chronic Fatigue Syndrome. Neuroimage Clin. 11, 530–537.
Benjamini, Y., Hochberg, Y., 1995. Controlling the false discovery rate: a practical and powerful approach to multiple testing. J. Roy. Stat. Soc. Ser. B 57, 289–300.
Biswal, B., Kunwar, P., Natelson, B., 2011. Cerebral blood flow is reduced in chronic fatigue syndrome as assessed by arterial spin labeling. J. Neurol. Sci. 301, 9–11.
Boissoneault, J., Letzen, J., Lai, S., O'Shea, A., Craggs, J., Robinson, M.E., Staud, R., 2016a. Abnormal resting state functional connectivity in patients with chronic fatigue syndrome: an arterial spin-labeling fMRI study. Magn. Reson. Imaging 34, 603–608.
Boissoneault, J., Letzen, J., Lai, S., Robinson, M.E., Staud, R., 2016b. Static and dynamic functional connectivity in patients with chronic fatigue syndrome: use of arterial spin labelling fMRI. Clin. Physiol. Funct. Imaging. http://dx.doi.org/10.1111/cpf.12393. (Epub ahead of print PMID: 27678090).
Caseras, X., Mataix-Cols, D., Giampietro, V., Rimes, K.A., Brammer, M., Zelaya, F., Chalder, T., Godfrey, E.L., 2006. Probing the working memory system in chronic fatigue syndrome: a functional magnetic resonance imaging study using the n-back task. Psychosom. Med. 68, 947–955.
Caseras, X., Mataix-Cols, D., Rimes, K., Giampietro, V., Brammer, M., Zelaya, F., Chalder, T., Godfrey, E., 2008. The neural correlates of fatigue: an exploratory imaginal fatigue provocation study in chronic fatigue syndrome. Psychol. Med. 38, 941–951.
Cook, D., Lange, G., DeLuca, J., Natelson, B., 2001. Relationship of brain MRI abnormalities and physical functional status in CFS. Int. J. Neurosci. 107, 1–6.
Cook, D., O'Connor, P., Lange, G., Steffener, J., 2007. Functional neuroimaging correlates of mental fatigue induced by cognition among chronic fatigue syndrome patients and controls. NeuroImage 36, 108–122.
Coste, C.P., Sadaghiani, S., Friston, K.J., Kleinschmidt, A., 2011. Ongoing brain activity fluctuations directly account for intertrial and indirectly for intersubject variability in Stroop task performance. Cereb. Cortex 21, 2612–2619.
Fan, L., Li, H., Zhuo, J., Zhang, Y., Wang, J., Chen, L., Yang, Z., Chu, C., Xie, S., Laird, A.R., Fox, P.T., Eickhoff, S.B., Yu, C., Jiang, T., 2016. The human Brainnetome Atlas: a new brain atlas based on connectional architecture. Cereb. Cortex 26, 3508–3526.
Fukuda, K., Straus, S.E., Hickie, I., Sharpe, M.C., Dobbins, J.G., Komaroff, A., 1994. The chronic fatigue syndrome: a comprehensive approach to its definition and study. Ann. Intern. Med. 121, 953–959.
Gay, C.W., Robinson, M.E., Lai, S., O'Shea, A., Craggs, J.G., Price, D.D., Staud, R., 2016. Abnormal resting-state functional connectivity in patients with chronic fatigue syndrome: results of seed and data-driven analyses. Brain Connect. 6, 48–56.
Goldberger, A.L., Amaral, L.A., Hausdorff, J.M., Ivanov, P., Peng, C.K., Stanley, H.E., 2002. Fractal dynamics in physiology: alterations with disease and aging. Proc. Natl. Acad. Sci. U. S. A. 99 (Suppl. 1), 2466–2472.
Hager, B., Yang, A.C., Brady, R., Meda, S., Clementz, B., Pearlson, G.D., Sweeney, J.A., Tamminga, C., Keshavan, M., 2017. Neural complexity as a potential translational biomarker for psychosis. J. Affect. Disord. 216, 89–99.
Holgate, S., Komaroff, A., Mangan, D., Wessely, S., 2011. Chronic fatigue syndrome: understanding a complex illness. Nat. Rev. Neurosci. 12, 539–544.
Jenkinson, M., Bannister, P., Brady, M., Smith, S., 2002. Improved optimization for the robust and accurate linear registration and motion correction of brain images. NeuroImage 17, 825–841.
Keenan, P., 1999. Brain MRI abnormalities exist in chronic fatigue syndrome. J. Neurol. Sci. 171, 1–2.
Kielar, A., Deschamps, T., Chu, R.K., Jokel, R., Khatamian, Y.B., Chen, J.J., Meltzer, J.A., 2016. Identifying dysfunctional cortex: dissociable effects of stroke and aging on resting state dynamics in MEG and fMRI. Front. Aging Neurosci. 8, 40.
Kim, B.H., Namkoong, K., Kim, J.J., Lee, S., Yoon, K.J., Choi, M., Jung, Y.C., 2015. Altered resting-state functional connectivity in women with chronic fatigue syndrome. Psychiatry Res. 234, 292–297.
Lange, G., Wang, M., DeLuca, J., Natelson, B., 1998. Neuroimaging in chronic fatigue syndrome. Am. J. Med. 105, 50S–53S.
Lange, G., DeLuca, J., Maldjian, J., Lee, H.-J., Tiersky, L., Natelson, B., 1999. Brain MRI abnormalities exist in a subset of patients with chronic fatigue syndrome. J. Neurol. Sci. 171, 3–7.
de Lange, F., Kalkman, J., Bleijenberg, G., Hagoort, P., Sieberen, P., van der Werf, S., Van der Meer, J., Toni, I., 2004. Neural correlates of the chronic fatigue syndrome - an fMRI study. Brain 127, 1948–1957.
de Lange, F., Kalkman, J., Bleijenberg, G., Hagoort, P., van der Meer, J., Toni, I., 2005. Gray matter volume reduction in the chronic fatigue syndrome. NeuroImage 26, 777–781.
Lange, G., Steffener, T., Cook, D., Bly, B., Christodoulou, C., Liu, W.-C., DeLuca, J., Natelson, B., 2005. Objective evidence of cognitive complaints in Chronic Fatigue Syndrome: a BOLD fMRI study of verbal working memory. NeuroImage 26, 513–524.
Leung, H.C., Skudlarski, P., Gatenby, J.C., Peterson, B.S., Gore, J.C., 2000. An event-related functional MRI study of the stroop color word interference task. Cereb. Cortex

10, 552–560.
Liu, T.T., Frank, L.R., Wong, E.C., Buxton, R.B., 2001. Detection power, estimation efficiency, and predictability in event-related fMRI. NeuroImage 13, 759–773.
Mizuno, K., Tanaka, M., Tanabe, H.C., Joudoi, T., Kawatani, J., Shigihara, Y., Tomoda, A., Miike, T., Imai-Matsumura, K., Sadato, N., Watanabe, Y., 2015. Less efficient and costly processes of frontal cortex in childhood chronic fatigue syndrome. Neuroimage Clin. 9, 355–368.
Mizuno, K., Kawatani, J., Tajima, K., Sasaki, A.T., Yoneda, T., Komi, M., Hirai, T., Tomoda, A., Joudoi, T., Watanabe, Y., 2016. Low putamen activity associated with poor reward sensitivity in childhood chronic fatigue syndrome. Neuroimage Clin. 12, 600–606.
Nguyen, T., Johnston, S., Clarke, L., Smith, P., Staines, D., Marshall-Gradisnik, S., 2017. Impaired calcium mobilization in natural killer cells from chronic fatigue syndrome/myalgic encephalomyelitis patients is associated with transient receptor potential melastatin 3 ion channels. Clin. Exp. Immunol. 187, 284–293.
Okada, T., Tanaka, M., Kuratsune, H., Watanabe, Y., Sadato, N., 2004. Mechanisms underlying fatigue: a voxel-based morphometric study of chronic fatigue syndrome. BMC Neurol. 4, 14–19.
Perrin, R., Embleton, K., Pentreath, V., Jackson, A., 2010. Longitudinal MRI shows no cerebral abnormality in chronic fatigue syndrome. Br. J. Radiol. 83, 419–423.
Pincus, S.M., 2006. Approximate entropy as a measure of irregularity for psychiatric serial metrics. Bipolar Disord. 8, 430–440.
Puri, B.K., Jakeman, P.M., Agour, M., Gunatilake, K.D., Fernando, K.A., Gurusinghe, A.I., Treasaden, I.H., Waldman, A.D., Gishen, P., 2012. Regional grey and white matter volumetric changes in myalgic encephalomyelitis (chronic fatigue syndrome): a voxel-based morphometry 3 T MRI study. Br. J. Radiol. 85, e270–273.
Ray, C., Phillips, L., Weir, W.R., 1993. Quality of attention in chronic fatigue syndrome: subjective reports of everyday attention and cognitive difficulty, and performance on tasks of focused attention. Br. J. Clin. Psychol. 32 (Pt 3), 357–364.
Reyes, M., Nisenbaum, R., Hoaglin, D.C., Unger, E.R., Emmons, C., Randall, B., Stewart, J.A., Abbey, S., Jones, J.F., Gantz, N., Minden, S., Reeves, W.C., 2003. Prevalence and incidence of chronic fatigue syndrome in Wichita, Kansas. Arch. Intern. Med. 163, 1530–1536.
Richman, J.S., Moorman, J.R., 2000. Physiological time-series analysis using approximate entropy and sample entropy. Am. J. Physiol. Heart Circ. Physiol. 278, H2039–2049.
Shan, Z.Y., Kwiatek, R., Burnet, R., Del Fante, P., Staines, D.R., Marshall-Gradisnik, S.M., Barnden, L.R., 2016. Progressive brain changes in patients with chronic fatigue syndrome: a longitudinal MRI study. J. Magn. Reson. Imaging 44, 1301–1311.
Shan, Z.Y., Kwiatek, R., Burnet, R., Del Fante, P., Staines, D.R., Marshall-Gradisnik, S.M., Barnden, L.R., 2017. Medial prefrontal cortex deficits correlate with unrefreshing sleep in patients with chronic fatigue syndrome. NMR Biomed. http://dx.doi.org/10.1002/nbm.3757. (Epub 2017 Jun 29, PMID: 28661067).
Shan, Z.Y., Finegan, K., Bhuta, S., Ireland, T., Staines, D.R., Marshall-Gradisnik, S.M., Barnden, L.R., 2018. Brain Connect. http://dx.doi.org/10.1089/brain.2017.0549. (Epub 2018 Jan 3, PMID: 29152994).
Sokunbi, M.O., 2014. Sample entropy reveals high discriminative power between young and elderly adults in short fMRI data sets. Front. Neuroinform. 8, 69.
Takahashi, T., Cho, R.Y., Murata, T., Mizuno, T., Kikuchi, M., Mizukami, K., Kosaka, H., Takahashi, K., Wada, Y., 2009. Age-related variation in EEG complexity to photic stimulation: a multiscale entropy analysis. Clin. Neurophysiol. 120, 476–483.
Tanaka, M., Sadato, N., Okada, T., Mizuno, K., Sasabe, T., Tanabe, H.C., Saito, D.N., Onoe, H., Kuratsune, H., Watanabe, Y., 2006. Reduced responsiveness is an essential feature of chronic fatigue syndrome: a fMRI study. BMC Neurol. 6, 9.
Tie, Y., Suarez, R.O., Whalen, S., Radmanesh, A., Norton, I.H., Golby, A.J., 2009. Comparison of blocked and event-related fMRI designs for pre-surgical language mapping. NeuroImage 47, T107–115.
Ware Jr., J.E., Kosinski, M., Bayliss, M.S., McHorney, C.A., Rogers, W.H., Raczek, A., 1995. Comparison of methods for the scoring and statistical analysis of SF-36 health profile and summary measures: summary of results from the Medical Outcomes Study. Med. Care 33, As264-279.
Wortinger, L.A., Endestad, T., Melinder, A.M., Oie, M.G., Sevenius, A., Bruun Wyller, V., 2016. Aberrant resting-state functional connectivity in the salience network of adolescent chronic fatigue syndrome. PLoS One 11, e0159351. http://dx.doi.org/10.1371/journal.pone.0159351.
Wortinger, L.A., Glenne Oie, M., Endestad, T., Bruun Wyller, V., 2017. Altered right anterior insular connectivity and loss of associated functions in adolescent chronic fatigue syndrome. PLoS One 12, e0184325. http://dx.doi.org/10.1371/journal.pone.0184325.
Zeineh, M.M., Kang, J., Atlas, S.W., Raman, M.M., Reiss, A.L., Norris, J.L., Valencia, I., Montoya, J.G., 2015. Right arcuate fasciculus abnormality in chronic fatigue syndrome. Radiology 274, 517–526.